Ind. Eng. Chem. Res. **1998,** *37,* 405−411

MATERIALS AND INTERFACES

Effect of pH of Precipitation on the Preparation of High Surface Area Aluminas from Nitrate Solutions

Klaus Hellgardt* and David Chadwick

Imperial College of Science, Technology and Medicine, Department of Chemical Engineering and Chemical Technology, London SW7 2BY, U.K.

The influence of the pH of precipitation on the morphology and the nitrate retention of aluminas prepared from nitrate solutions has been investigated. pH control causes the BET surface area of γ-alumina to vary between 180 and 410 m^2/g and determines the extent of microporosity within the aluminas. Particle sizes derived from XRD data are compared to values quoted in the open literature. Strong retention of nitrate ion was found for precipitation at pH below the PZC; at the same time, the precipitate density was sharply lowered. However, nitrate retention did not adversely affect the development of surface area following heat treatment.

Introduction

Alumina is prepared on a commercial scale by the Bayer process (e.g. Emons et al., 1978) and is employed in a variety of scientific and commercial fields ranging from abrasives, ceramics, catalysts to medical applications. γ-Alumina, defined as a low temperature alumina $Al_2O_3 \cdot nH_2O$ with $0 < n < 0.6$ and dehydrated below 600 °C (Ginsberg et al., 1957), is frequently used as a support material in heterogeneous catalysis due to its low cost, thermal stability, high surface area, and significant interaction with deposited transition metals. However, special applications require preparation from pure sources such as aluminum salts or alkoxides.

Alumina can be precipitated batch- or semibatchwise by mixing two appropriate solutions. This causes the pH of precipitation to vary considerably. The composition of the ligand sphere of the Al^{3+} ions in aqueous solution is strongly influenced by the pH of the solution (Dudeney et al., 1991). Olation, or the formation of “ol-” bridges between two or more metal atoms, is the principal condensation process. The properties of the resulting precipitate reflect the amount of crosslinking which in turn is influenced by the ratio of hydroxo/aquo ligands in the coordination sphere of the metal ion (Livage et al., 1988). The primary particles of the precipitate will exhibit a surface charge, again depending on the pH of the precipitation solution, which affects the amount of agglomeration that occurs during a given residence time. Furthermore, foreign ions (or counterions) may also be retained via adsorption or incorporation depending on the surface charge.

Comprehensive reviews (Lippens and Steggerda, 1970; Trimm and Stanislaus, 1986) have been published on the preparation and transformation of aluminas. Much less has been reported on the effect of precipitation parameters such as pH, temperature and residence time on the final structure and properties of the obtained material, although it is clear from the considerations above that the pH of precipitation will have a strong effect on the structure of the precipitate and hence on the morphology of the final product. Nixon et al. (1987) have shown a strong influence of the pH of precipitation (pH of reaction solution) on the viscosity of the precipitate; however, they did not address the final properties of the prepared materials (after drying). The morphologies of some aluminas prepared from inorganic precursor solutions have been reported: Johnson and Mooi (1968) prepared boehmite from $AlCl_3$. Vogel et al. (1984) used ammonium bicarbonate as precipitant yielding a new crystalline phase. Ono et al. (1983) applied a novel pH swing process using sodium aluminate as precipitant and reported morphological properties such as BET surface areas and average pore sizes, mainly obtained for a specific pH of precipitation. Here we report the effect of the pH of precipitation on the final properties of aluminas prepared from nitrate solutions by *continuous* precipitation. In particular, we demonstrate that surface area, pore size, density, and nitrate ion retention strongly reflect the pH of precipitation.

Experimental Section

γ-Aluminas were prepared in a laboratory scale apparatus for continuous precipitation, Figure 1 (Hellgardt and Chadwick, 1994). The system allows control of pH, temperature, agitation speed (mixing), and residence time (aging time) during the precipitation process. To avoid contamination, system parts are made only of Pyrex glass, Teflon and stainless steel. The nitrate solution and the precipitant (NH_4OH) are brought into contact using a double-jet injector. This allows for intensive mixing in a very small contact zone (approximately 8 mm^3). The pH was measured just above the jet and was controlled by manual adjustment of the ratio of the pumping speeds of the two peristaltic

---

* To whom correspondence should be addressed. Present address: Department of Chemical Engineering, Loughborough University, Loughborough, Leicestershire LE11 3TU, U.K. Telephone: 01509 22 2518. Fax: 01509 22 3923. E-mail: k.hellgardt@lboro.ac.uk.

S0888-5885(97)00591-5 CCC: $15.00

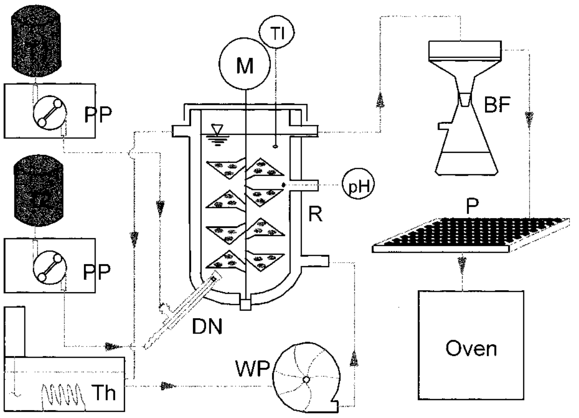

T = Tank
PP = Peristaltic Pump
Th = Thermostat
DN = Double Nozzle
WP = Water Pump
R = Reactor
M = Stirrer
pH = Electrode
TI = Thermocouple
BF = Buchner Funnel
P = Perforated Plate

Figure 1. Flow diagram of the designed precipitation system.

pumps. The jacketed reactor vessel is continuously stirred with a purpose-built stirrer which allows for turbulent radial mixing with minimal axial dispersion. This gives rise to a rather narrow residence time distribution; a residence time of 0.5 min^{-1} was used for the precipitation process in the present experiments. The precipitate rises continuously within the vessel and is discharged and filtered. The initial precipitates obtained during pH stabilization were discarded. The collected precipitate (obtained at constant pH) was then washed with boiling distilled, deionized water and subsequently distributed onto perforated steel plates. Drying in an air circulated oven at 120 °C for 12 h produces uniform pellets which were crushed to below 250 μm diameter for analysis.

The BET surface area and pore volume distributions were determined using a Micromeritics ASAP 2000 instrument. Prior to analysis, the samples were degassed under vacuum at 573 K for 12 h. The densities of the prepared aluminas after drying at 393 and 573 K were recorded using a He displacement pycnometer by Micromeritics.

XRD was carried out on a Philips PW1710 automated powder diffractometer using Cu Kα radiation. The 2θ angle was varied from 0° to up to 120° in steps of 0.02. The alumina samples were crushed to below 50 μm and distributed onto silicon wafers using acetone. The Si $\langle 111 \rangle$ reflection was used as internal standard.

Temperature programmed desorption (TPD) was carried out up to 1273 K in a purpose-built reactor system (Chadwick and O'Malley, 1988). An attached RGA (residual gas analyser) was used to monitor the desorption and decomposition products.

Results and Discussion

Effect of pH of Precipitation on the BET Surface Area and the Pore Size Distribution. Alumina was prepared by continuous precipitation at constant pH and 298 K from a 0.52 M nitrate solution (based on the cation concentration), using a 5% ammonia solution. A series of aluminas was produced in which the pH of precipitation was varied between 6.0 and 9.0 in steps of 0.5.

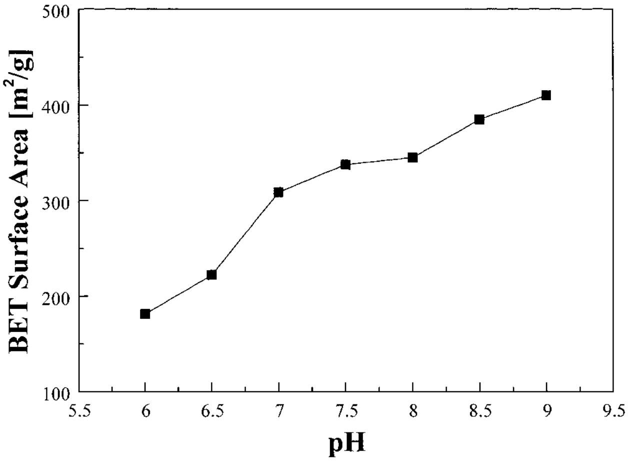

Figure 2. BET surface areas of aluminas as a function of the pH of precipitation.

The BET surface areas of the precipitated aluminas are plotted in Figure 2 as a function of their pH of precipitation. The BET surface area increases continuously from around 180 m^2/g at pH 6.0 to 410 m^2/g at pH 9.0. These data are in good agreement with those reported by Vogel et al. (1984), who found 302 m^2/g at a pH of 8.0 by applying a similar precipitation method. Precipitation from aluminium sulfate solution at a pH of 9.0 and subsequent drying at 393 K for 6 h resulted in a BET surface area of 300 m^2/g according to Lippens and Steggerda (1970). Johnson and Mooi (1968) determined the BET surface areas of their boehmite, precipitated from chloride solution at a pH of 8.0, to be 339 m^2/g after calcination. Ono et al. (1971) observed a BET surface area of 318 m^2/g for pseudo-boehmite precipitated from sodium aluminate and aluminum nitrate solution at a pH of 8.0 and a temperature of 373 K. Comparison of the above data indicates that whereas the pH of precipitation is important, the precursor aluminum species, be it sulfate, nitrate, chloride, or even hydrogen carbonate, appears to have very little effect on the final surface area of the prepared γ-alumina. In the present investigation, the average pore size of the precipitated γ-alumina was determined as a function of the pH of precipitation, Figure 3. It can be noted that the average pore size increases continuously from about 1.6 nm at pH 6.0 to some 7 nm at a pH of 7.5. However, there seems to exist an upper average pore size limit for aluminas precipitated above pH 7.5. The average pore size values for the aluminas precipitated in alkaline medium correlate again reasonably well with previously reported data: Ono et al. (1971) determined 5.9 nm as a modal pore diameter at pH 8.0. The value determined by Vogel et al. (1984), 4.8 nm, is somewhat lower than the present value. Johnson and Mooi (1968) observed major pore sizes of between 4.0 and 7.0 nm depending on the crystallite size.

As the average pore size is usually a good reflection of the actual crystallite size for micro/mesoporous systems, it can be concluded that, apparently, no change in the rate of aggregation occurs in alkaline medium. This has been stressed by Ono et al. (1971), who argue that dissolution and redispersion occur predominantly

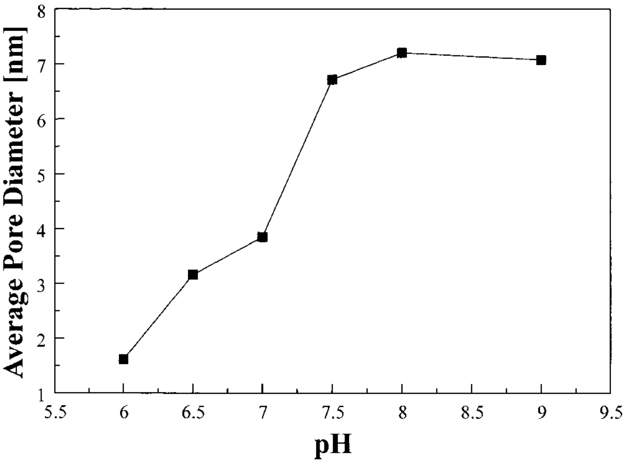

Figure 3. Average pore sizes of aluminas as a function of the pH of precipitation.

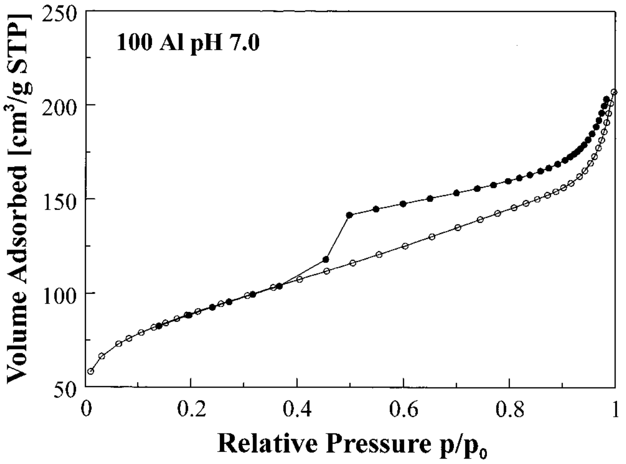

Figure 4. Ad-/desorption isotherms for alumina precipitated at pH 7.0.

in acidic media leading to very small crystallite sizes, while the growth of pseudo-boehmite crystallites in alkaline media is only governed by the aging time. The aging time in our case is equal to the residence time, which was constant for all the prepared aluminas.

The recorded adsorption and desorption isotherms for all prepared aluminas show significant hysteresis at relative pressures p/p_0 above 0.38. Figure 4 gives as an example of the recorded ad-/desorption isotherms for alumina precipitated at pH 7.0, which are typical of a type IV physisorption isotherm (Sing et al., 1985), the pronounced “knee” at low relative pressures being indicative of the presence of microporosity. The hysteresis loop is a Type H4 loop, often associated with narrow slitlike pores. The desorption pore volume plots for the aluminas prepared at pH 6.0, 7.0, 8.0, and 9.0 are given in Figure 5. All samples show a very narrow pore size distribution. The maximum pore volume of alumina precipitated at pH 6.0 lies in the micropore region, <2 nm. With increasing pH of precipitation, the maximum pore size shifts into the mesopore region. The pore size distributions of the aluminas prepared at pH 8.0 and 9.0 do not exhibit significant changes compared to that of the alumina prepared at pH 7.0. This is consistent with the constant average pore size, noted earlier. The peak maximum in the pore volume plots for the aluminas prepared at pH 8.0 and 9.0 lie around 4 nm, which now very well corresponds to the data

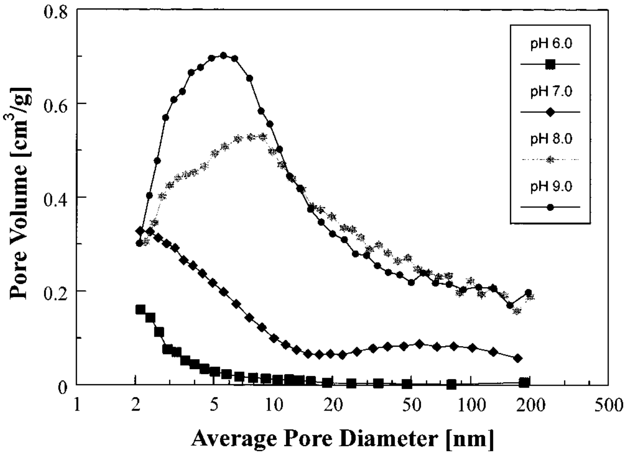

Figure 5. Adsorption pore volume plot for precipitated alumina.

obtained by other researchers. The higher values of the average pore diameter in the case of high pH of precipitation result from the contribution of larger pores to the average which become more significant with increasing pH of precipitation. A similar result was observed when comparing the adsorption pore volume plots, Figure 6. This graph gives clear evidence of the increasing pore volume as a function of the increasing pH of precipitation. Again the alumina prepared at pH 6.0 shows N_2 adsorption mainly in the micropore region, while the aluminas prepared at pH 8.0 and 9.0 establish an adsorption maximum between 2 and 10 nm.

To quantify the micropore volumes of the prepared aluminas, t-plots were constructed using the Harkins–Jura equation (Harkins and Jura, 1944)

$$t = \sqrt{\frac{13.99}{\left(0.0340 - \log\left(\frac{p}{p_0}\right)\right)}} \qquad \text{(I)}$$

to calculate the statistical thickness of the adsorbate from the relative pressures (p/p_0). The thickness values used in the least-square analysis were chosen between 0.35 and 0.5 nm. The constants were determined using a nonporous reference material. Figure 7 shows the regression analysis of the plots of adsorbed volume versus the statistical thickness. A slightly positive or negative deviation from the standard isotherm was observed for all catalysts which may be due to some minor porosity of the standard sample (above statistical thickness of 0.5 nm). From the regression analysis performed on the data in Figure 7, the micropore volumes of the alumina samples were determined and indicated a nearly linear decrease of the micropore volume as a function of the pH of precipitation, Figure 8. For alumina prepared at pH 6.0 the micropore volume comprises of almost 40% of the total pore volume of the sample. In the case of the alumina prepared at pH 9.0 the micropore volume amounts only to ca. 0.7%. We also noted that the color of the vacuum dried samples varied from dirty yellow (pH 6.0) to bright white (pH 9.0) which could be an indication for different particle or pore sizes. Furthermore, during the drying process shrinkage of the pellets occurred, with the alumina prepared at pH 6.0 shrinking by about 50 vol % and the alumina prepared at pH 9.0 shrinking only by ca. 5 vol %.

To gain further insight into the structure of the dried (373 K) and the heat-treated aluminas (573 K, vacuum),

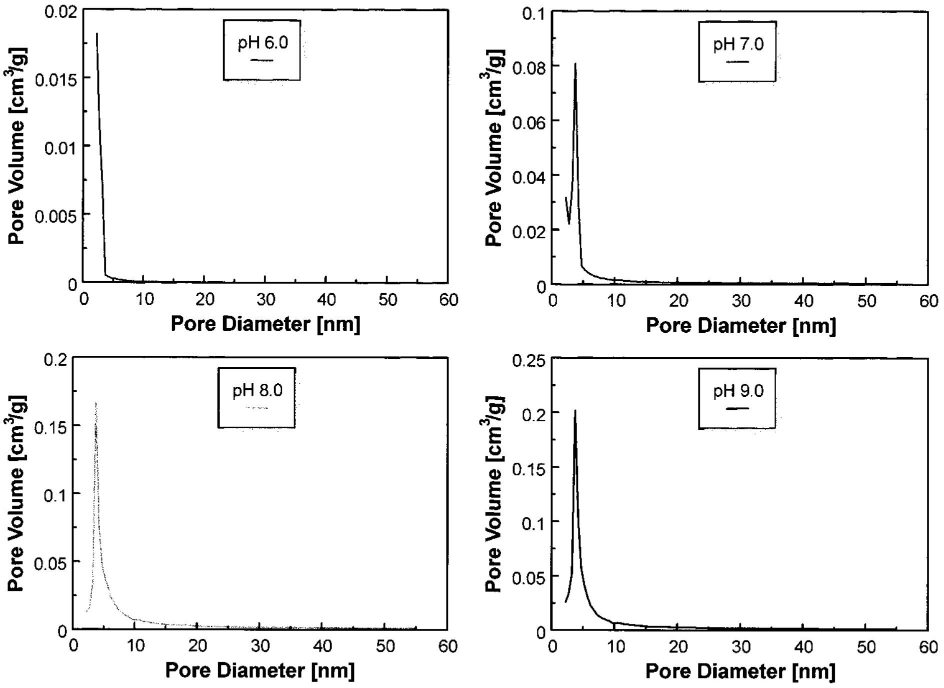

Figure 6. Desorption pore volume plots for precipitated alumina.

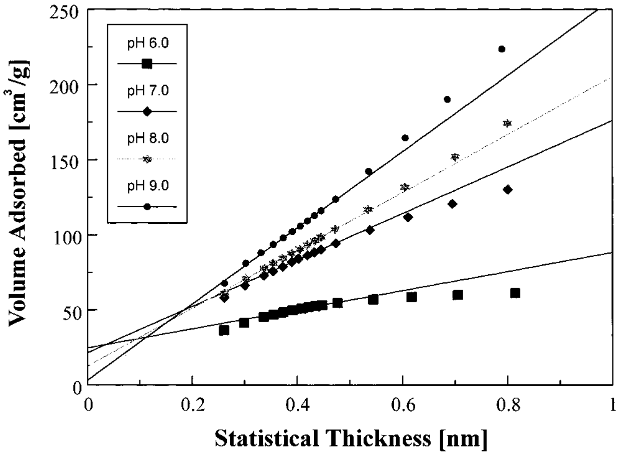

Figure 7. *t*-Plots of precipitated alumina.

selected samples were subjected to XRD analysis. The XRD patterns of two dried aluminas, precipitated at pH 6.0 and 9.0, are given in Figure 9. Seven or eight peaks can be discriminated, the observed patterns corresponding solely to boehmite. The alumina prepared at pH 9.0 appears to be more crystalline than the sample prepared at pH 6.0. A similar diffraction pattern is shown by Vogel et al. (1984) for boehmite prepared at pH 8.0 using ammonium bicarbonate and dried at 473 K. These authors still observe this pattern (boehmite) after heat treatment at 623 K.

The X-ray diffraction patterns of the heat-treated (573 K, vacuum) aluminas precipitated at pH 6.0, 7.0, 8.0, and 9.0 are given in Figure 10. The diffraction patterns are almost identical and are typical of nearly amorphous γ-alumina. Vogel et al. (1984) observed a similar diffraction pattern after calcination of boehmite at 923 K. At this point we can make a clear distinction between the boehmite prepared by Vogel et al. (1984) and our material. It seems that Vogel et al. (1984) have produced well crystallized boehmite which transforms at approximately 723 K to γ-alumina. The transformation of our product into γ-alumina at a considerably lower temperature of 573 K suggests that our precipitation process yields gelatinous boehmite or pseudo-boehmite. These two boehmite modifications cannot be easily discriminated using XRD techniques. Similar transformation temperatures have been reported by Lippens and Steggerda (1970) and Trimm and Stanislaus (1986).

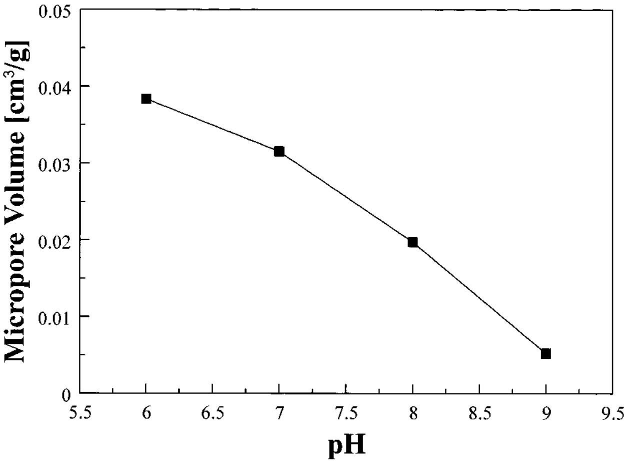

Figure 8. Micropore volume as a function of pH for precipitated aluminas.

The crystallite sizes calculated for the heat-treated samples (γ-alumina) vary only slightly, from 2.8 to 4.3 nm (based on the main reflection of γ-alumina at $2\theta = 66.82°$, corresponding to the $\langle 440 \rangle$ plane). The crystallite sizes for the dried samples (boehmite) were calculated using the reflection at $2\theta = 38.33°$, corresponding to the $\langle 140{,}031 \rangle$ plane. The boehmite precipitated at pH 6.0 yielded a crystallite size of 2.2 nm while the boehmite prepared at pH 9.0 exhibited some 3.1 nm. These values are in extremely good agreement with those obtained by Ono et al. (1971) for very short aging times.

The particle size of the dried and the heat treated samples are reasonably close given the limitations of

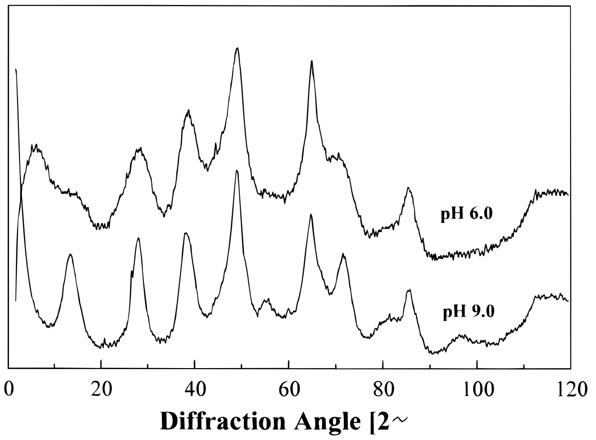

Figure 9. Diffraction patterns of alumina prepared at pH 6.0 and 9.0.

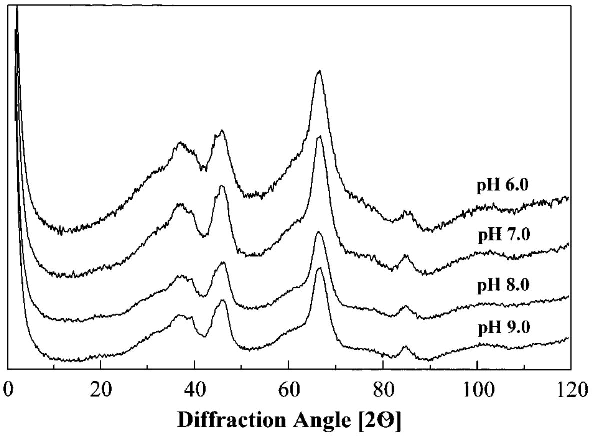

Figure 10. Diffraction patterns of vacuum-dried alumina prepared at pH 6.0, 7.0, 8.0, and 9.0.

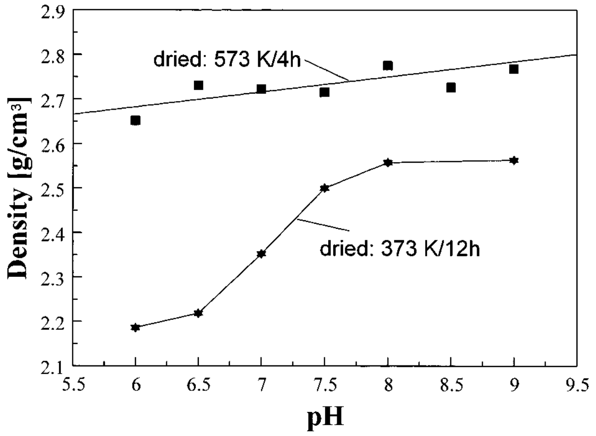

Figure 11. Densities of precipitated aluminas after heat treatment.

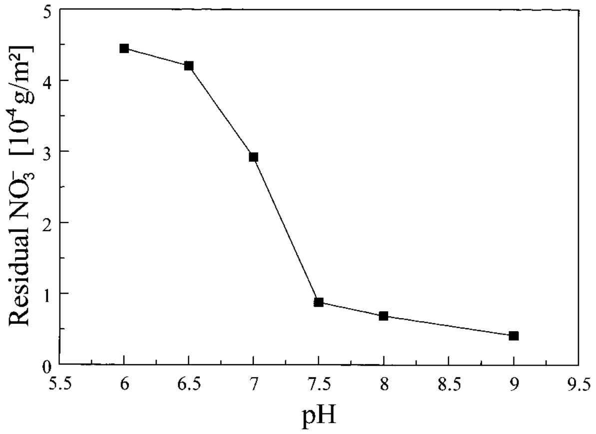

Figure 12. Residual nitrate content of precipitated aluminas.

calculations based on the Scherrer formula (Klug and Alexander, 1974), and there seems to be no strong influence of the pH of precipitation on the crystallite size. Clearly, this suggests that the BET surface areas are not governed by the individual particle/crystallite sizes but are instead governed by the extent of agglomeration and dissolution of the primary particles. This process is strongly dependent on the pH of precipitation. Partial dissolution of the initial aluminum hydroxide (particularly at low pH) will lead to increased agglomeration and hence to a lower BET surface area and a higher degree of microporosity.

The measured skeletal densities of all the aluminas were found to be much lower than the literature value of 3.01 g/cm^3 for boehmite (CRC Handbook, 1987). Figure 11 shows the densities of the dried aluminas as a function of the pH for the two different drying temperatures (393 and 573 K). A distinct density change was observed for the aluminas dried at 393 K. This occurs at a pH around 7.2, where the density increases considerably from 2.2 to 2.55 cm^3/g, and approximately coincides with the PZC (point of zero charge) of γ-alumina and boehmite at 7.5 and 7.5−7.7 respectively (Parks, 1965). This rather surprising behavior can only mean that either there are two structural regimes or that a substantial amount of foreign ions (NO_3^-, OH^-) or molecules (H_2O) have been incorporated into the framework of the prepared boehmite or adsorbed onto the large precipitate surface area. The XRD patterns point to the latter explanation. This is discussed further below. A slightly increasing density as a function of pH with overall higher values was determined for the same series dried at 573K in vacuum. For these samples there is no hint of S-shaped behavior. The XRD shows an increasingly crystalline appearance and the density is closer to the true boehmite value.

Effect of the pH of Precipitation on Nitrate Retention. TPD of an acidic- (pH 6.0) and a basic- (pH 9.0) prepared alumina was carried out in order to determine the decomposition products released during the drying process at 573 K. Strong NO_x (N_2O, NO) evolution occurred around 523 K in the case of the acidic-prepared alumina which can be assigned solely to the decomposition of nitrate species. H_2O desorption was observed over the temperature range from 373 to 673 K. The basic alumina only exhibited a broad water desorption peak from 373 to 673 K with no evidence for nitrate related species.

Figure 12 shows the nitrate content of the precipitated aluminas (adjusted for their respective BET surface areas) as a function of the pH of precipitation. The nitrate content decreases with increasing pH of precipitation and exhibits a point of inflection around pH 7.2. These results demonstrate that substantial amounts of foreign anions or counteranions (here NO_3^-) can be retained by the precipitates either in the boeh-

Table 1. Comparison of Boehmite Precipitated at pH 6.0: Effect of Washing

	boehmite A, normal washing procedure	boehmite B, extensive washing, 24 h
pH of precipitation	6.0	6.0
initial nitrate content (wt %)	8	0.08
BET surface area (m^2/g)	181.6	247.7
av pore size (nm)	1.62	2.53
micropore vol (cm^3/g)	0.0384	0.0299
density (cm^3/g)	2.652	2.817

mite structure or adsorbed on the large available surface area. This occurs predominantly when the surface charge is positive (pH lower than the PZC). It is interesting to note that the maximum nitrate retention (assuming close packed monolayer adsorption on the surface of the alumina and a coverage area of one nitrate ion to be 0.3 nm^2) would amount to around 5.8 wt % nitrate retention in the case of the alumina prepared at pH 6.0. This is in reasonable agreement with the determined value of 8 wt %, given the assumptions, and suggests that the nitrate ion is mainly adsorbed. Similar effects have been noted and exploited in the preparation of catalysts (Ng and Gulari, 1983). Even severe washing does not remove these ions completely as has been observed by other researchers for different ions (Montanaro and Guilhot, 1989). Aluminas heat treated at 573 K do not contain any appreciable amount of nitrate due to the decomposition of the residual nitrate at 530 K as shown by the TPD results.

To address whether nitrate retention has any effect on the morphological properties of the precipitated aluminas, boehmite precipitated at a pH of 6 was subjected to rigorous washing with boiling deionized water for 24 h. During this procedure a considerable amount of precipitate was lost. The remaining boehmite possessed a very low residual nitrate content of ca. 800 ppm, Table 1.

BET surface area, average pore size, and density are higher for the alumina with the reduced nitrate content. As expected, during the prolonged washing with deionized boiling water at pH 7, dissolution and reprecipitation as well as particle growth occur. This leads to values for the BET surface area and the other properties of the material which are closer to those determined for the alumina prepared at pH 6.5, in agreement with the predicted shift of the structural properties. Overall the results suggest that water and nitrate retention do not seriously impair the structural properties of precipitated alumina after heat treatment.

Conclusions

The BET surface area of precipitated alumina is rather independent of the precursor material (nitrate, chloride, sulfate, hydrogen carbonate) when prepared at the same pH and similar aging conditions. A wide range of BET surface areas (180−410 m^2/g) and average pore sizes (<2−7 nm) can be achieved for aluminas prepared from nitrate solutions by tight control of the precipitation parameters (particularly the pH of precipitation). Under the applied conditions an upper limit for the average pore size seems to exist. A further increase of pore size above 7 nm is only possible by variation of the aging time (increase agglomeration time and hence particle size). Aluminas develop a narrow pore size distribution, the major pore size being in the range of the particle indicative of interparticle spaces. The construction of *t*-plots is a fairly good means of calculating the micro pore volumes of microporous/mesoporous systems. Micropores are dominant in aluminas prepared under acidic conditions while mainly mesopores are observed under alkaline conditions. The transformation from boehmite to γ-alumina can readily take place at temperatures as low as 573 K in vacuum. Particle sizes derived from XRD and BET data appear to be in reasonable agreement.

Nitrate retention is significant at a pH of precipitation below the PZC (pH 7.2 in this case). However, the residual nitrate is completely decomposed at 573 K. Results indicate that the morphology of aluminas derived from low pH precipitation is not affected by the considerable amount of nitrate retained.

Acknowledgment

The authors would like to acknowledge the financial support of this project by the European Union and the British Council.

Literature Cited

Chadwick, D.; O'Malley, P. J. R. Propan-2-ol Adsorption and Decomposition on Zinc-Oxide Promoted by Alkali-Metal. *J. Chem. Soc., Faraday Trans.* **1987**, *183*, 2227−2241.

CRC Handbook of Chemistry and Physics, Physical Constants of Inorganic Compounds; West, R. C., Astle, M. J., Beyer, W. H., Eds.; CRC Press Inc.: Boca Raton, FL, 1987; p B-68.

Dudeney, A. W. L.; Ghani, M. A.; Kelsall, G. H., Zhang, L. Alumina Powders from Aqueous Precipitation, Particle Extraction and Calcination. *Fine Ceramic Powders*, British Ceramic Proceedings 47; Institute of Ceramics: Shelton, Stoke-on-Trent, U.K., 1991; pp 13−24.

Emons, H. H, Brautigam, G., Hellmold, P., Holldorf, H., Kummel, R., Martens, H. *Grundlagen der technischen anorganischen Chemie*; VEB: Leipzig, Germany, 1978.

Ginsberg, H.; Hüttig, W.; Strunk-Lichtenberg, G. The Influence of the Starting Material on the Crystalline Forms Arising in the Thermal Decomposition and Conversion of Aluminum Hydroxides. I. The Crystalline Forms of the Thermal Decomposition of γ-Aluminum Hydroxide. *Z. Anorg. Allg. Chem.* **1957**, *293*, 33−46.

Harkins, W. D.; Jura, G. Surface of Solids. X. Extension of the Attractive Energy of a Solid into an Adjacent Liquid Film, the Decrease of Energy with Distance, and the Thickness of Films. *J. Am. Chem. Soc.* **1944**, *66*, 919−927.

Hellgardt, K.; Chadwick, D. Factors Affecting the Preparation of Potassium Promoted, Iron Based Coprecipitated Catalysts. *Proc. 1994 IChemE Res. Event* **1994**, *2*, 595−597.

Johnson, M. F. L.; Mooi, J. The Origin and Types of Pores in Some Alumina Catalysts. *J. Catal.* **1968**, *10*, 342−354.

Klug, H. P.; Alexander, L. E. *X-Ray Diffraction Procedures*; John Wiley & Sons Inc.: New York, 1974.

Lippens, B. C.; Steggerda, J. J. Active Alumina. In *Physical and Chemical Aspects of Adsorbents and Catalysts*; Linsen, B. G., Ed.; Academic Press: London and New York, 1970; pp 171−211.

Livage, J.; Henry, M.; Sanchez, C. Sol-Gel Chemistry of Transition-Metal Oxides. *Prog. Solid State Chem.* **1988**, *18*, 259−341.

Montanaro, L.; Guilhot, B. Preparation of Microspheres from Alumina-Zirconia Sol. *Ceram. Bull.* **1989**, *68*, 1017−1020.

Ng, K. Y. S.; Gulari, E. Molybdena on Titania. I. Preparation and Characterisation by Raman and Fourier Transform Infrared Spectroscopy. *J. Catal.* **1985**, *92*, 340−354.

Nixon, P. R.; White, J. L.; Hem, S. L. Investigation of pH-Dependent Gel Structure in Amorphous Carbonate-Containing Aluminum Hydroxide by Viscosimetry, Fibre Optic Doppler

Anemometry, and Freeze Fracture/Freeze Etch Scanning Electron Microscopy. *J. Colloid Interface Sci.* **1987**, *120*, 312−319.

Ono, T.; Ohguchi, Y.; Togari, O. Control of the Pore Structure of Porous Alumina. In *Preparation of Catalysts III*; Poncelet, G., Grange P., Jacobs, P. A., Eds.; Elsevier Science Publishers B. V.: Amsterdam, 1983; pp 631−641.

Parks, G. A. The Isoelectric Points of Solid Oxides, Solid Hydroxides, and Aqueous Hydroxo Complex Systems. *Chem. Rev.* **1965**, *65*, 177−198.

Sing, K. S. W.; Everett, D. H.; Haul, R. A. W.; Moscou, L.; Pierotti, R. A.; Rouquérol, J.; Siemieniewska, T. Reporting Physisorption Data for Gas Solid Systems with Special Reference to the Determination of Surface-Area and Porosity (Recommendations 1984). *Pure Appl. Chem.* **1985**, *57*, 603−619.

Trimm, D. L.; Stanislaus, A. The Control of Pore Size in Alumina Catalyst Supports: A Review. *Appl. Catal.* **1986**, *21*, 215−238.

Vogel, R. F.; Marcelin, G.; Kehl, W. L. The Preparation of Controlled Pore Alumina. *Appl. Catal.* **1984**, *12*, 237−248.

Received for review August 26, 1997
Revised manuscript received October 21, 1997
Accepted October 27, 1997[⊗]

IE970591A

[⊗] Abstract published in *Advance ACS Abstracts,* December 15, 1997.